



## Evidence for K-rich terranes on Vesta from impact spherules

Jean-Alix J-A Barrat, Marcel Bohn, P. Gillet, A. Yamaguchi

### ► To cite this version:

Jean-Alix J-A Barrat, Marcel Bohn, P. Gillet, A. Yamaguchi. Evidence for K-rich terranes on Vesta from impact spherules. *Meteoritics and Planetary Science*, 2009, 44 (3), pp.359-374. insu-00401913

**HAL Id: insu-00401913**

**<https://hal-insu.archives-ouvertes.fr/insu-00401913>**

Submitted on 26 Feb 2013

**HAL** is a multi-disciplinary open access archive for the deposit and dissemination of scientific research documents, whether they are published or not. The documents may come from teaching and research institutions in France or abroad, or from public or private research centers.

L'archive ouverte pluridisciplinaire **HAL**, est destinée au dépôt et à la diffusion de documents scientifiques de niveau recherche, publiés ou non, émanant des établissements d'enseignement et de recherche français ou étrangers, des laboratoires publics ou privés.

## Evidence for K-rich terranes on Vesta from impact spherules

J. A. BARRAT<sup>1,2\*</sup>, M. BOHN<sup>1,2</sup>, PH. GILLET<sup>3</sup>, and A. YAMAGUCHI<sup>4</sup>

<sup>1</sup>Université Européenne de Bretagne, France

<sup>2</sup>CNRS UMR 6538 (Domaines Océaniques), U.B.O.-I.U.E.M., Place Nicolas Copernic, 29280 Plouzané Cedex, France

<sup>3</sup>Laboratoire des Sciences de la Terre, CNRS UMR 5570, Université de Lyon, Ecole Normale Supérieure de Lyon,

46 Allée d'Italie, 69364 Lyon Cedex 7, France

<sup>4</sup>Antarctic Meteorite Research Center, National Institute of Polar Research, 1-9-10 Kaga, Itabashi, Tokyo 173-8515, Japan

\*Corresponding author. E-mail: [barrat@univ-brest.fr](mailto:barrat@univ-brest.fr)

(Received 29 May 2008; revision accepted 07 November 2008)

**Abstract**—The howardite-eucrite-diogenite (HED) clan is a group of meteorites that probably originate from the asteroid Vesta. Some of them are complex breccias that contain impact glasses whose compositions mirror that of their source regions. Some K-rich impact glasses (up to 2 wt% K<sub>2</sub>O) suggest that in addition to basalts and ultramafic cumulates, K-rich rocks are exposed on Vesta's surface. One K-rich glass (up to 6 wt% K<sub>2</sub>O), with a felsic composition, provides the first evidence of highly differentiated K-rich rocks on a large asteroid. They can be compared to the rare lunar granites and suggest that magmas generated in a large asteroid are more diverse than previously thought.

### INTRODUCTION

The early stages of planetary formation in the solar system involved a large population of small to medium-sized objects, colliding with each other to form the major planets (Weidenschilling 2000). Some of them melted and differentiated into a metallic core, an ultramafic mantle, and a basaltic crust. Most of these primitive differentiated bodies have now disappeared, such that the formation and degree of differentiation of these primitive small and medium-sized planets is still a matter of debate (McCoy et al. 2006). Today, only a handful of such small planets are still orbiting in the asteroid belt, between Mars and Jupiter (Sunshine et al. 2004). Vesta, one of them, is differentiated with an intact internal structure, and is covered by basalts and pyroxenites. It is probably the source of one of the most important group of differentiated meteorites, namely the howardite, eucrite, and diogenite (HED) suite (e.g., Drake 2001). Eucrites are basaltic rocks that display magmatic textures indicating formation as lava flows or intrusions. Diogenites are orthopyroxene-rich cumulates that formed in a plutonic environment. Diogenites and eucrites are often breccias consisting of a mixture of crystal debris and rock fragments reflecting many impact events on the surface of their parent body. Howardites are more complex breccias made chiefly of eucritic and diogenitic clasts. They occasionally contain impact melt clasts, glass beads or debris (e.g., Noonan 1974). Some of these glasses could have been ballistically transported from distant impact sites and mixed to the

regolith before the impact responsible for the launch of the meteorites from the parent body. Thus, these glasses may originate from terrains not directly sampled by typical HED meteorites, and could therefore provide, in addition to future remote sensing observations, a complementary view of the composition of the surface of Vesta.

Here, we report on the petrography and the major element geochemistry of impact spherules and glass fragments from seven howardites. We will show that some of the glasses cannot be explained by impact melting of typical HED lithologies. Some K-rich impact glasses (up to 2 wt% K<sub>2</sub>O) suggest that in addition to basalts and ultramafic cumulates, K-rich rocks are exposed on Vesta.

### ANALYTICAL METHODS

We determined the major-element compositions of the glasses by electron microprobe analysis using a Cameca Camebax at Hawaii's Institute of Planetology, Honolulu (Bununu and Kapoeta), a JEOL JXA8200 at National Institute of Polar Research, Tokyo (Yamato [Y-] 7308 and 791208), and a Cameca SX100 at Ifremer, Plouzané (LaPaz Icefield [LAP] 04838, Northwest Africa [NWA] 1664 and 1769). All analyses used wavelength dispersive spectrometers at 15 KV accelerating voltage, 10–12 nA beam current, and a spot size ranging from 10 to 30 µm. In the case of phases in the porphyritic glasses (NWA 1664, NWA 1769 and LAP 04838), and for the felsic area in a NWA 1664 spherule, 1 µm spots

were used. Minerals (wollastonite [Si, Ca], orthoclase [K], albite [Na], apatite [P]), oxide ( $\text{MnTiO}_3$  [Mn, Ti],  $\text{Al}_2\text{O}_3$  [Al],  $\text{Fe}_2\text{O}_3$  [Fe],  $\text{Cr}_2\text{O}_3$  [Cr],  $\text{FeS}_2$  [S], etc.), and metal standards (Ni) were used for calibration. In order to avoid the heterogeneity effects induced by small crystals or inclusions, the compositions of the glasses given here are averages of 2 to 30 analyses depending of the size of the object. Analyses of inclusions or rims of the spherules have been excluded from the averages.

Raman spectra were acquired with a Labram HR800 model of Jobin-Yvon Horiba spectrometer equipped with a microscope for collection of backscattered Raman signal and equipped with a CCD detector. The spectrometer was used in backscattering geometry. The laser beam (514.5 nm exciting lines of a Spectra Physics® Ar<sup>+</sup> laser) was focused through microscope objectives ( $\times 100$ ) down to a 1 micrometer spot on sample and the backscattered light was collected through the same objective.

## RESULTS

Seven glass-bearing howardites (Bununu, Kapoeta, LAP 04838, NWA 1664 and 1769, Y-7308 and Y-791208) have been selected. In all the samples, glassy objects are heterogeneously dispersed in a fine-grained clastic matrix, together with diagenitic and eucritic fragments. They generally consist of spherules (or beads) and more frequently angular fragments.

### Petrography

#### Spherules

Spherules are generally ellipsoidal in shape, and commonly about 500  $\mu\text{m}$  in diameter (Figs. 1 and 2). They are often broken. A variety of textures are revealed by scanning electron microscopy. Some are fully glassy (Fig. 1 A and B), while others are vitrophyric containing olivine or pyroxene crystals in a glassy matrix. The morphologies of the crystals are similar to those obtained experimentally in fast cooled basaltic or ultramafic melts (e.g., Donaldson et al. 1975; Arndt et al. 1984; Faure et al. 2003). Three types of olivine morphology occur in the spherules: lattice olivine (Fig. 1C), fiber olivine (Fig. 2A), and chains of skeletal crystals (Figs. 2C, 3, and 4). Dendritic (Fig. 4A) pyroxenes are common. The variety of crystal shapes are clearly related to cooling rate and degree of undercooling of the melts (e.g., Donaldson et al. 1975; Arndt et al. 1984; Faure et al. 2003) and not surprisingly, point to very fast cooling rate values (in the order of a few K/s or faster). Furthermore, droplets or grains of metal (typically Fe 98 wt%, Ni 2 wt%) and troilite are present in most of the spherules, and are normally less than 30  $\mu\text{m}$  in diameter. Detailed chemical mapping performed on selected spherules shows that some of them are coated by minute grains of sulfides and phosphates that are

unfortunately too small to be properly analyzed by electron microprobe (Fig. 5). Similar coatings have been previously described on impact spherules from the Moon, and are interpreted as condensates from a vapor cloud formed with the spherules (Ruzicka et al. 2000). Furthermore, the spherules are not always chemically uniform. In addition to possible small scale heterogeneities in the melts, which can be strongly obscured by the development of dendritic crystals, some of the spherules have rims nearly devoid of Na and K ( $\text{Na}_2\text{O}$  and  $\text{K}_2\text{O} < 0.02$  wt%, see Fig. 5), which suggests that they have lost a significant portion of their alkalis during their flight and cooling.

Three unusual spherules were analyzed during the course of this study. The first one, found in NWA 1769 (Fig. 6), displays an orthopyroxene nucleus coated with an homogeneous glass that contains rare tiny Ca-rich plagioclase grains. The orthopyroxene crystal is unzoned, and has a typically diagenitic composition ( $\text{En}_{74.6}\text{Wo}_{2.2}\text{Fs}_{23.2}$ ,  $\text{FeO}/\text{MnO} = 30$ , see Table 1). This would appear to be a remnant of the target, which has melted to form the glass. The second one is a broken spherule found in NWA 1664 (Figs. 3 and 4). This object displays a vitrophyric texture with chains of skeletal olivine and dendritic clinopyroxene crystals. Interestingly, this fragment is a composite, as it consists of three different types of glassy areas (Table 1), all cross-cut by the olivine crystals. The fragment is dominated by a Na-poor, K-rich glass ( $\text{Mg\#} [=100 \times \text{Mg}/(\text{Mg} + \text{Fe}), \text{atomic}] = 53.1$ ,  $\text{Na}_2\text{O} = 0.20$  wt%,  $\text{K}_2\text{O} = 1.41$  wt%), mostly in the internal part of the spherule. The external rim of the spherule is Na-rich and K-poor ( $\text{Mg\#} = 47.0$ ,  $\text{Na}_2\text{O} = 1.21$  wt%,  $\text{K}_2\text{O} = 0.06$  wt%). Finally, a felsic glass is located in a 15  $\mu\text{m}$  thick strip (red in the K map; Fig. 3). The glassy nature of the felsic component is confirmed by Raman spectra (Fig. 7). A few K rich patches are seen in the core of the broken spherule (Fig. 3) and correspond either to interstitial glass areas enriched in K after the crystallization of olivine and pyroxene, or areas slightly contaminated by the felsic melt. These K-rich patches should not be overemphasized, and their scarcity confirms that the different melts did not mix together significantly inside the spherule. Furthermore, the limits between the felsic and the mafic glasses are sharp, and indicate that the melts involved were largely immiscible. The last one, found again in NWA 1664 (#1664B7,2S) contains two different mafic glasses, both K-rich (Table 1 and Fig. 8). Again, the boundaries between the two different glasses are sharp.

#### Fragments of Glass

Angular fragments of glass, sometimes vesicular, are more frequent than spherules (Figs. 9 and 10). They are generally small (typically a few hundreds of  $\mu\text{m}$ ), but some as large as 2 cm have been previously reported in NWA 1664 (Kurat et al. 2003). They can be fully glassy, vitrophyric, to crystal-rich, and many display textures very similar to those of the spherules. Crystal-rich glasses display a wide range of

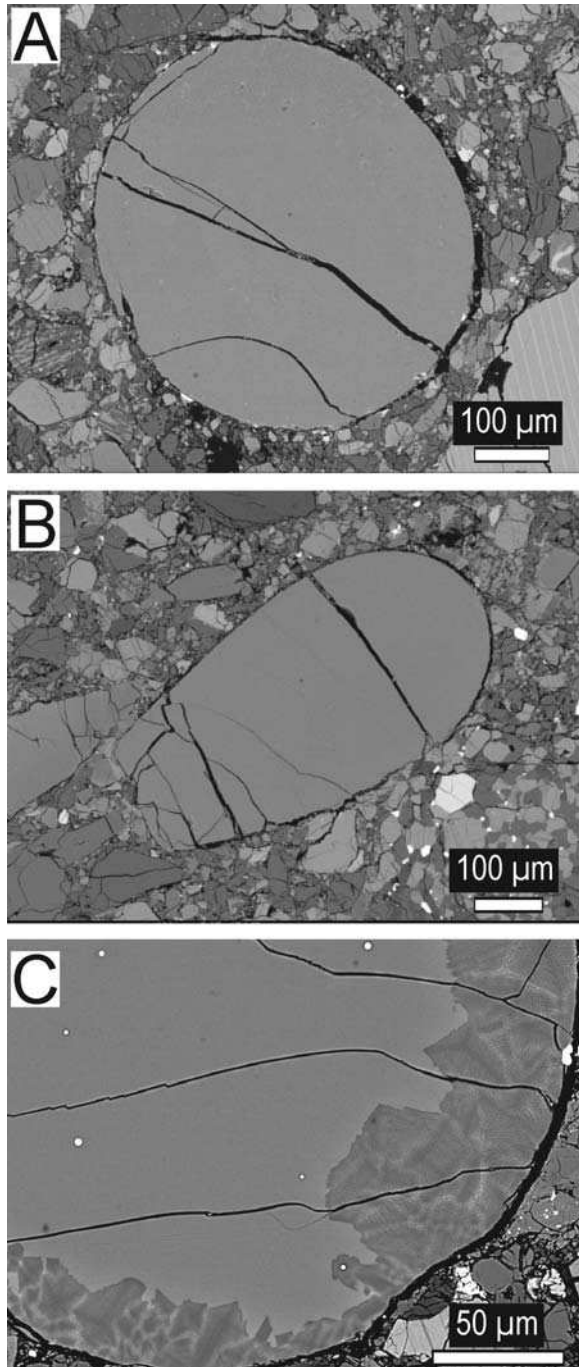


Fig. 1. Backscattered electron images of glass spherules from howardites. A and B) Vitreous spherules from NWA 1769. C) Vitreous spherule from Y-7308 with lattice olivine in its rim. Notice the droplets of metal (white).

features. Here we provide only a short description of two of them which display different mineral assemblages.

The first one occurs in NWA 1664 (clast 1664B3, 3). This clast contains low-Ca pyroxene and olivine phenocrysts in glass (Fig. 10B, and Table 1). Minor phases are metal ( $\text{Fe}_{98}\text{Ni}_2$ ) and troilite. The pyroxene crystals are unlike typical diagenitic

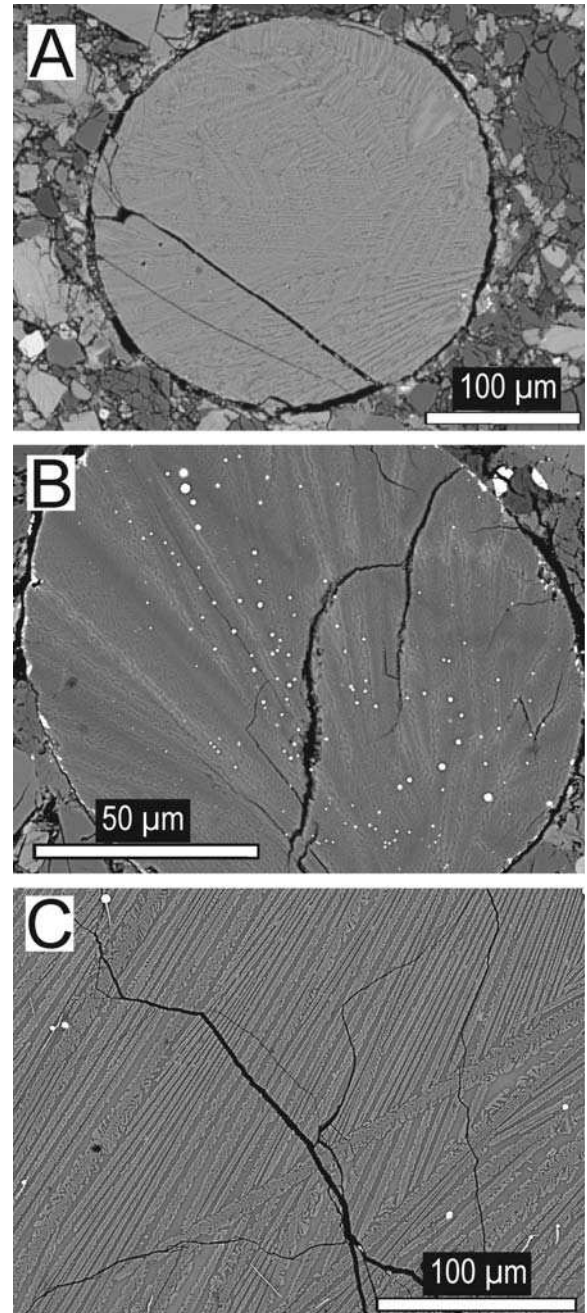


Fig. 2. Backscattered electron images of glass spherules from howardites. A) Spherule from NWA 1769 with fibre and lattice olivine. B) Spherule from Y-7308 with radiating olivine chains and pyroxene crystals (?). Notice the droplets of metal (white). C) Quenched-texture in a spherule from Y-7308.

pyroxenes (e.g., Fowler et al. 1994; Mittlefehldt 1994). They are zoned from  $\text{En}_{80.1}\text{Wo}_{2.1}\text{Fs}_{17.8}$  in the cores to  $\text{En}_{69.0}\text{Wo}_{6.6}\text{Fs}_{24.4}$  in the rims, and are Al and Cr-rich ( $\text{Al}_2\text{O}_3 = 1.5\text{--}4.0$  wt%,  $\text{Cr}_2\text{O}_3 = 0.95\text{--}2.1$  wt%). Such unusual concentrations have been previously measured in pyroxenes from fast cooled lunar basalts and impactites (Engelhardt et al. 1989; Barrat et al. 2003). Olivine crystals are unzoned ( $\text{Fo}_{64}$ ).



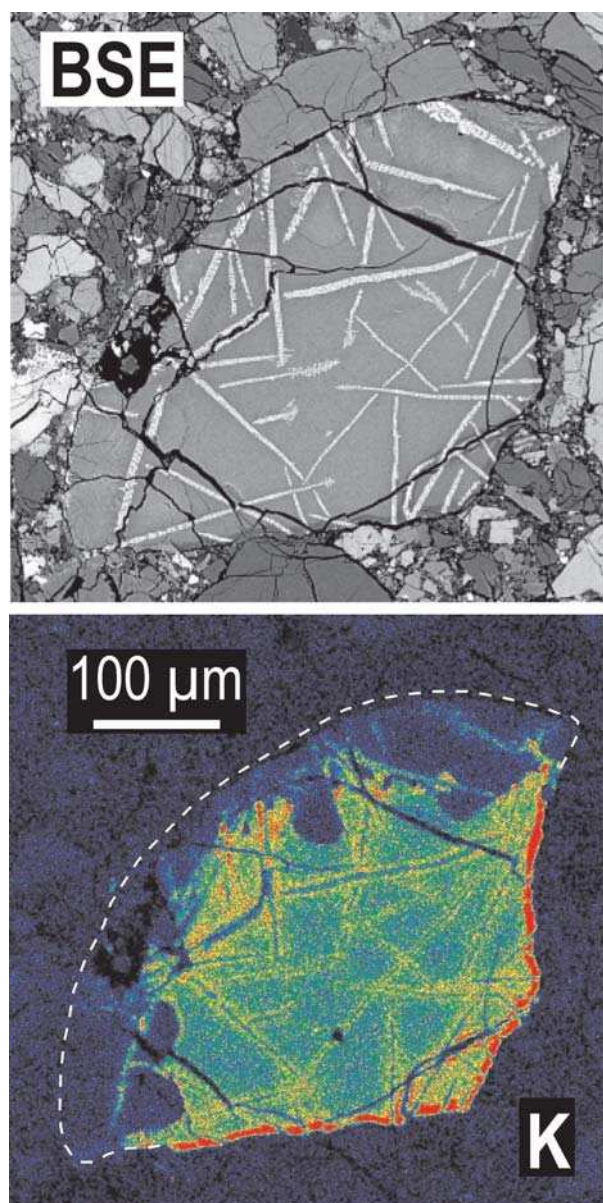


Fig. 3. Backscattered electron image and K map of the broken impact spherule found in NWA 1664 that contains a felsic glass. The shape of the felsic area before the fragmentation of the spherule is unknown. This glass is located in a 15 µm thick strip (red in the K map) in contact with a Na-poor, K-rich mafic glass ( $Mg\# = 53.1$ ,  $Na_2O = 0.20$  wt%,  $K_2O = 1.41$  wt%) that composes apparently the internal part of the spherule. Chains of skeletal olivine crosscut the boundaries between the different glasses.

The second clast is from LAP 04838 (clast LAP, 2). The glass contains two types of crystals (Fig. 10C and Table 1). The first, most abundant, type consists of plagioclase and equilibrated pyroxene debris which are clearly derived from a eucritic precursor. These angular fragments do not have the morphology of unmelted remnants sometimes found in impact melts (shock features are missing here). Thus, they are more likely regolith-derived and enclosed by the

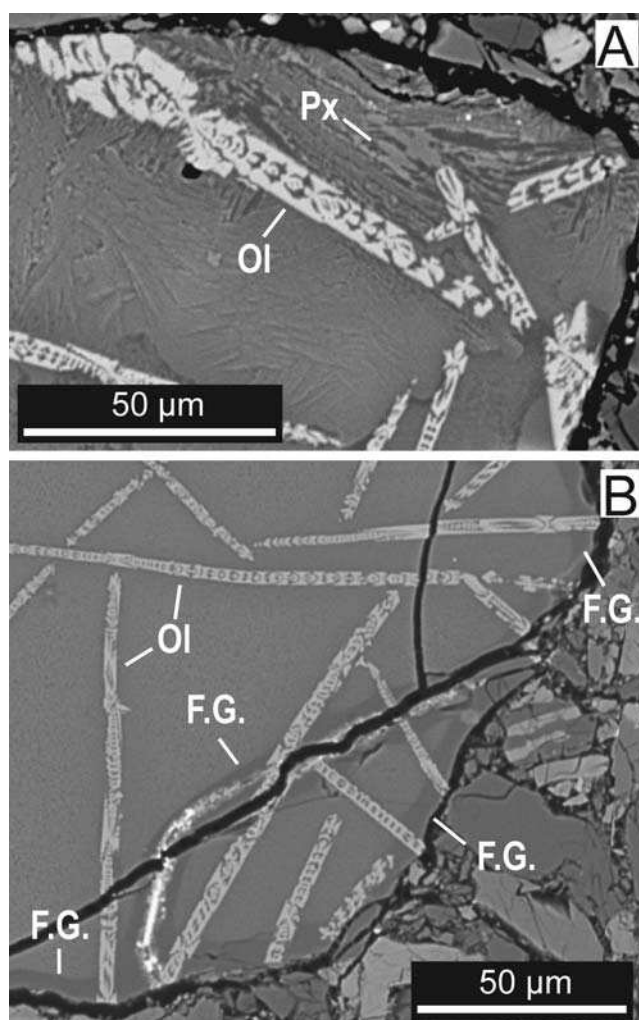


Fig. 4. Backscattered electron images of the broken impact spherule found in NWA 1664 that contains a felsic glass. A) Chains of skeletal olivine crystals (Ol) and dendritic pyroxene (px). B) Chains of skeletal olivine (Ol) crosscut the strip of felsic glass (dark grey, F.G.).

melt at a late stage. The second consists of pyroxenes (50 µm in length), sometimes skeletal, which have grown from the glass. These crystals are strongly zoned from low-Ca cores ( $En_{63}Wo_7Fs_{30}$ ) to pigeonitic rims ( $En_{32}Wo_{29}Fs_{39}$ ), with again a strong Al enrichment ( $Al_2O_3$  from 4 to 11.8 wt%).

### Chemistry

Because it is not always possible to accurately reverse-calculate the composition of the original melt represented by the crystal-rich glass fragments, we have restricted our study to the spherules and aphyric glass fragments. Sixty-one glassy clasts or spherules have been analyzed here (Table 1), and their average compositions are compared to howardites, eucrites and diogenites in Fig. 11. Three chemically different types of glasses have been recognized:

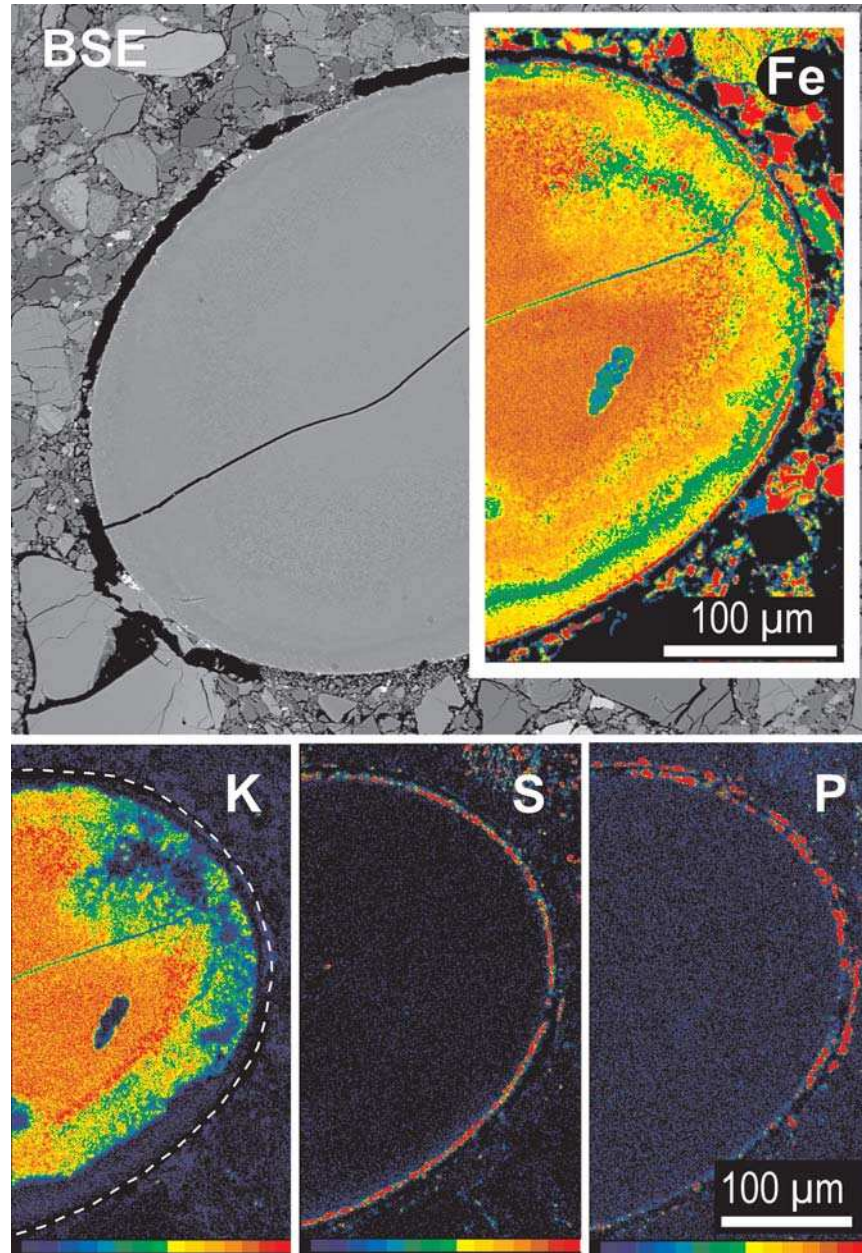


Fig. 5. Backscattered electron image and maps of Fe, K, S, and P of an heterogeneous spherule found in NWA 1769 that contains a rim devoid of K and a coating made of fine sulfide and phosphate grains.

1. Glasses from Bununu, Kapoeta, Y-7308, and Y-791208, including data from Noonan (1974), Yagi et al. (1978), Klein and Hewins (1979), Noonan et al. (1980), Delaney et al. (1982), and Ikeda and Takeda (1984), display a wide range of composition with Mg# from 41 to 72, which overlap those of eucrites and howardites. These glasses are K-poor, with  $K_2O$  generally less than 0.1 wt%.
2. Mafic glasses found in NWA 1664, NWA 1769, and LAP 04838 display a range of compositions similar to the previous K-poor glasses, with Mg# from 32 to 73,

although in some cases they have significantly lower Ca and Na than expected for typical HED lithologies. More importantly, they are unusually K-rich, with  $K_2O$  concentrations ranging from 0.17 to 2.33 wt%. High-K abundances were previously noticed in glasses from NWA 1664 (Kurat et al. 2003), Luotolax (Delaney et al. 1982) and from the Malvern howardites (Noonan 1974; Desnoyers and Jérôme 1977). These K abundances are much higher than those reported for most of the HED meteorites, which contain in most cases less than 0.1 wt%  $K_2O$ .



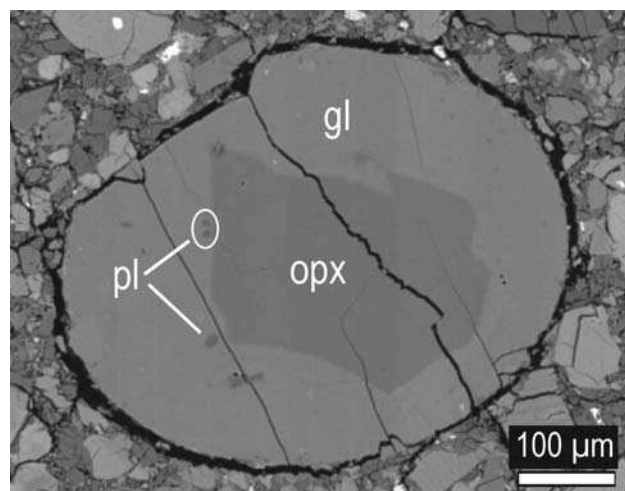


Fig. 6. Backscattered electron images of a composite impact spherule found in NWA 1769 with an orthopyroxene nucleus (opx). The glass (gl) contains small plagioclase grains (pl).

3. The silica-rich glass found in a fragment of a spherule from NWA 1664, displays high  $K_2O$  abundances ranging from 4 to 6.12 wt%. The compositions correspond to a high-K, low Na monzogranite. CIPW norms indicate a small excess of  $Al_2O_3$  (normative corundum from 0.8 to 2.91%), which could be the result of a loss of alkalis during impact.

## DISCUSSION

Glasses found in howardites can be produced by two different processes, either volcanic fire-fountaining (Delaney et al. 1982) or impact melting. We agree with previous studies that a volcanic origin is unlikely, and these glasses, including the K-rich ones, have certainly formed upon impacts from lithologies exposed on 4 Vesta (e.g., Noonan 1974; Hewins and Klein 1978; Yagi et al. 1978; Klein and Hewins 1979; Noonan et al. 1980; Ikeda and Takeda 1984; Boesenberg et al. 2007): schlieren (e.g., Kurat et al. 2003), and meteoritic Fe-Ni metal have been often observed in spherules and glassy fragments. In addition, the occurrence of a remnant of a diagenetic orthopyroxene in the core of a spherule strengthens this interpretation.

The occurrence of composite spherules containing different types of glasses (spherules 1664B1,1S and 1664B7,2S) could suggest at first glance that silicate liquid immiscibility (SLI) played a role during their formation. However, we do not favor the involvement of such a process during the cooling of the spherules for at least three reasons:

1. If SLI was operative, composite spherules should be relatively common; instead, such objects are more the exception than the rule.
2. Experimental works have shown that pairs of liquids generated by SLI exhibit contrasting chemical

compositions (Thompson et al. 2007); the chemical differences between the mafic glasses found in the spherules #1664B1,1S and #1664B7,2S (Table 1) are much less marked.

3. Although silica-rich melts similar to the felsic glass found in spherule #1664B1,1S can be produced by SLI, and are associated with low-Si, high Fe melts (Powell et al. 1980), their compositions are unlike the mafic melts found in the same spherule.

We suggest that the different glasses found in the rare composite spherules are more likely the remnants of heterogeneities in the target. Thus, as lunar impact glasses or terrestrial impactites and tektites, the compositions of the glasses found in howardites can provide strong constraints on the nature of their source regions.

The abundances of the least volatile elements straddle the fields drawn by the HED meteorites (Fig. 11, e.g.,  $Al_2O_3$ , CaO and  $TiO_2$  versus FeO/MgO). It can be emphasized that the range of the FeO/MnO ratios shown by the glasses and the HED meteorites are similar. Among the 61 mafic clasts and spherules we have analyzed during the course of the study, only 2 display values significantly different from the HED ones (1769A, 2S and 4S, see Table 1). The possible contamination of the glasses by metal from the impactor, or more likely the occurrence of an unusual lithology in the target (see below) can perfectly explain these outliers. However, the high K concentrations observed in impact glasses from NWA 1664 and NWA 1769 howardites, are astonishing.

Although hot-desert alteration can affect the composition of meteorites significantly, K abundances in the glassy clasts and spherules are certainly pristine. No K enrichment was detected close to the fractures or to the surface of both NWA 1664 and NWA 1769 howardites. The glassy objects were the only places where high K abundances were observed. The fusion crusts of both meteorites exhibit very low K concentrations, ruling out the possibility of a selective contamination of glasses. Furthermore, high K concentrations have been measured in glasses from the LAP 04838 howardite, a find from Antarctica, and more importantly, from the Luotolax and Malvern howardites (Noonan 1974; Desnoyers and Jérôme 1977; Delaney et al. 1982), and from the Macibini polymict eucrite (Buchanan et al. 2000), which are observed falls, and consequently have not suffered terrestrial weathering.

Clearly, the high-K concentrations displayed by some impact spherules require the contribution of an unusual component either from the impactor or the impacted area. The first hypothesis is unlikely because many of the impact glasses studied here contain much more K than all known meteorites. Therefore, their high-K concentrations are either linked to the compositions of the molten lithologies or generated by the shock processes. Potassium enrichments

Table 1. Averaged compositions of individual glassy fragments and spherules in howardites. Values are in wt%.

| #  | SiO <sub>2</sub> | TiO <sub>2</sub> | Al <sub>2</sub> O <sub>3</sub> | Cr <sub>2</sub> O <sub>3</sub> | FeO   | MnO  | MgO   | CaO   | Na <sub>2</sub> O | K <sub>2</sub> O | P <sub>2</sub> O <sub>5</sub> | Total  | Mg#   | FeO/MnO |
|--|------------------|------------------|--------------------------------|--------------------------------|-------|------|-------|-------|-------------------|------------------|-------------------------------|--------|-------|---------|
| Kapoeta, spherules (S) or glassy fragments (F)               |                  |                  |                                |                                |       |      |       |       |                   |                  |                               |        |       |         |
| BR3, S   | 50.36            | 0.43             | 9.13                           | 0.67                           | 18.32 | 0.51 | 14.21 | 7.25  | 0.36              | 0.03             | 0.04                          | 101.31 | 58.02 | 35.92   |
| K1-DB, S   | 50.42            | 0.56             | 11.10                          | 0.50                           | 18.25 | 0.48 | 10.71 | 8.77  | 0.21              | 0.16             | 0.01                          | 101.17 | 51.13 | 38.02   |
| C29, F   | 50.96            | 0.47             | 9.91                           | 0.65                           | 17.54 | 0.49 | 13.72 | 7.39  | 0.31              | 0.04             | 0.05                          | 101.53 | 58.23 | 35.80   |
| C1, F  | 48.19            | 0.63             | 11.54                          | 0.25                           | 20.87 | 0.62 | 9.23  | 9.32  | 0.19              | 0.01             | 0.09                          | 100.94 | 44.08 | 33.66   |
| C16, F   | 50.65            | 0.37             | 6.88                           | 0.66                           | 18.17 | 0.50 | 16.56 | 6.46  | 0.23              | 0.01             | 0.04                          | 100.53 | 61.90 | 36.34   |
| BR17, F  | 49.86            | 0.42             | 13.25                          | 0.47                           | 16.13 | 0.48 | 10.30 | 9.53  | 0.27              | 0.02             | 0.03                          | 100.76 | 53.22 | 33.60   |
| DC21, F  | 51.57            | 0.35             | 6.70                           | 0.65                           | 17.47 | 0.52 | 17.83 | 5.66  | 0.22              | 0.01             | 0.01                          | 100.99 | 64.54 | 33.60   |
| DC43, F  | 50.77            | 0.38             | 8.82                           | 0.69                           | 16.79 | 0.49 | 16.36 | 6.69  | 0.20              | 0.03             | 0.01                          | 101.23 | 63.45 | 34.27   |
| Bununu, spherules (S) or glassy fragments (F)                |                  |                  |                                |                                |       |      |       |       |                   |                  |                               |        |       |         |
| B1, S  | 50.73            | 0.39             | 8.58                           | 0.63                           | 17.47 | 0.52 | 14.81 | 6.92  | 0.25              | 0.03             | 0.02                          | 100.35 | 60.18 | 33.60   |
| B2, S  | 50.83            | 0.44             | 8.91                           | 0.61                           | 17.46 | 0.59 | 14.43 | 7.13  | 0.25              | 0.04             | 0.04                          | 100.73 | 59.57 | 29.59   |
| B3, F  | 49.73            | 0.74             | 12.58                          | 0.26                           | 18.84 | 0.62 | 7.42  | 10.86 | 0.39              | 0.08             | 0.05                          | 101.57 | 41.25 | 30.39   |
| B4, F  | 48.91            | 0.64             | 12.69                          | 0.22                           | 16.81 | 0.53 | 8.72  | 12.24 | 0.31              | 0.05             | 0.06                          | 101.18 | 48.03 | 31.72   |
| B5, F  | 51.00            | 0.52             | 13.74                          | 0.47                           | 15.36 | 0.53 | 8.73  | 10.20 | 0.34              | 0.03             | 0.04                          | 100.96 | 50.34 | 28.98   |
| B6, F  | 50.78            | 0.53             | 9.96                           | 0.52                           | 17.69 | 0.53 | 12.59 | 7.93  | 0.32              | 0.05             | 0.04                          | 100.94 | 55.92 | 33.38   |
| Y-7308, spherules (S) or glassy fragments (F)                |                  |                  |                                |                                |       |      |       |       |                   |                  |                               |        |       |         |
| 85-2, 1 F  | 51.81            | 0.22             | 6.00                           | 1.01                           | 16.12 | 0.50 | 19.62 | 4.72  | 0.06              | 0.01             |                               | 100.07 | 68.45 | 32.24   |
| 85-2, 2 F  | 52.47            | 0.18             | 4.80                           | 1.16                           | 15.77 | 0.51 | 21.49 | 3.61  | 0.04              | 0.12             |                               | 100.15 | 70.84 | 30.92   |
| 85-3, 1 S  | 51.04            | 0.26             | 6.03                           | 0.92                           | 16.23 | 0.51 | 19.30 | 4.86  | 0.13              | 0.01             |                               | 99.29  | 67.93 | 31.82   |
| 85-4, 1 F  | 52.35            | 0.17             | 4.40                           | 1.21                           | 15.58 | 0.50 | 21.90 | 3.49  | 0.07              | 0.12             |                               | 99.79  | 71.47 | 31.16   |
| 104-2, 1 S   | 53.83            | 0.21             | 4.50                           | 1.24                           | 15.04 | 0.56 | 20.70 | 3.68  | 0.13              | 0.08             |                               | 99.97  | 71.04 | 26.86   |
| 104-2, 2 F   | 52.17            | 0.22             | 5.97                           | 1.01                           | 15.33 | 0.54 | 19.61 | 4.70  | 0.14              | 0.17             |                               | 99.86  | 69.51 | 28.39   |
| 104-3, 1 S   | 51.60            | 0.22             | 5.88                           | 1.03                           | 16.18 | 0.52 | 19.74 | 4.64  | 0.12              | 0.07             |                               | 100.00 | 68.50 | 31.12   |
| Y-791208, glassy fragment (F)                                |                  |                  |                                |                                |       |      |       |       |                   |                  |                               |        |       |         |
| 81-2, 1 F  | 49.52            | 0.27             | 6.71                           | 0.93                           | 17.33 | 0.53 | 19.12 | 5.21  | 0.16              | 0.02             |                               | 99.80  | 66.29 | 32.70   |
| NWA 1664, fusion crust, spherules (S) or glassy fragment (F) |                  |                  |                                |                                |       |      |       |       |                   |                  |                               |        |       |         |
| 1664P, fusion crust  | 48.54            | 0.58             | 10.58                          | 0.40                           | 17.59 | 0.53 | 10.66 | 8.70  | 0.37              | 0.02             | 0.03                          | 98.00  | 51.92 | 33.19   |
| 1664P, 1 S   | 48.19            | 0.60             | 11.01                          | 0.47                           | 19.36 | 0.66 | 10.61 | 8.81  | 0.09              | 0.75             | 0.02                          | 100.57 | 49.41 | 29.33   |
| 1664P, 2 S   | 48.84            | 0.97             | 9.92                           | 0.58                           | 19.60 | 0.64 | 10.89 | 7.82  | 0.10              | 0.84             | 0.02                          | 100.22 | 49.76 | 30.63   |
| 1664P, 3 S   | 51.83            | 0.33             | 8.96                           | 0.45                           | 15.04 | 0.47 | 16.39 | 5.80  | 0.10              | 0.76             | 0.01                          | 100.14 | 66.00 | 32.00   |
| 1664P, 4 F   | 49.84            | 0.50             | 11.98                          | 0.49                           | 14.48 | 0.48 | 12.21 | 9.74  | 0.21              | 0.25             | 0.07                          | 100.25 | 60.05 | 30.17   |
| 1664P, 5 F   | 48.69            | 0.86             | 12.48                          | 0.28                           | 19.82 | 0.60 | 6.04  | 11.12 | 0.25              | 0.35             | 0.10                          | 100.59 | 35.22 | 33.03   |
| 1664B1, 1 F  | 49.68            | 0.58             | 11.78                          | 0.44                           | 17.74 | 0.53 | 9.23  | 9.97  | 0.21              | 0.44             | 0.04                          | 100.64 | 48.11 | 33.47   |
| 1664B1, 2 F  | 49.96            | 0.64             | 11.99                          | 0.43                           | 17.20 | 0.53 | 8.77  | 9.02  | 0.15              | 1.31             | 0.05                          | 100.05 | 47.62 | 32.45   |
| 1664B1, 3 F  | 49.15            | 1.19             | 12.89                          | 0.23                           | 19.12 | 0.54 | 5.19  | 11.32 | 0.30              | 0.68             | 0.11                          | 100.72 | 32.63 | 35.41   |
| 1664B1, 4 F  | 49.79            | 0.79             | 12.71                          | 0.31                           | 18.71 | 0.57 | 6.39  | 10.63 | 0.27              | 0.41             | 0.11                          | 100.69 | 37.85 | 32.82   |
| 1664B1, 5 F  | 49.11            | 0.57             | 12.03                          | 0.53                           | 16.15 | 0.55 | 10.55 | 8.98  | 0.16              | 1.07             | 0.04                          | 99.74  | 53.80 | 29.36   |
| 1664B2, 1 F  | 49.30            | 0.78             | 12.68                          | 0.36                           | 17.94 | 0.56 | 7.15  | 10.78 | 0.23              | 0.58             | 0.06                          | 100.42 | 41.53 | 32.04   |
| 1664B2, 2 F  | 49.00            | 0.73             | 12.06                          | 0.38                           | 17.89 | 0.56 | 7.45  | 9.40  | 0.18              | 1.46             | 0.07                          | 99.18  | 42.60 | 31.95   |
| 1664B3, 1 S  | 47.04            | 0.52             | 9.64                           | 0.55                           | 19.68 | 0.70 | 13.25 | 8.04  | 0.04              | 0.18             | 0.05                          | 99.69  | 54.55 | 28.11   |
| 1664B3, 2 S  | 51.20            | 0.61             | 9.91                           | 0.23                           | 19.24 | 0.65 | 8.02  | 8.61  | 0.24              | 0.68             | 0.10                          | 99.49  | 42.63 | 29.60   |
| 1664B4, 1 S  | 49.08            | 0.62             | 10.54                          | 0.39                           | 18.94 | 0.64 | 9.57  | 8.68  | 0.15              | 0.77             | 0.07                          | 99.45  | 47.40 | 29.74   |
| 1664B4, 2 S  | 49.11            | 0.58             | 10.03                          | 0.39                           | 19.29 | 0.66 | 10.28 | 8.44  | 0.14              | 0.54             | 0.07                          | 99.53  | 48.72 | 29.12   |
| 1664B5, 1S   | 49.55            | 0.54             | 9.82                           | 0.57                           | 18.33 | 0.62 | 11.75 | 7.25  | 0.09              | 0.93             | 0.04                          | 99.50  | 53.32 | 29.69   |
| 1664B5, 2S   | 48.84            | 0.65             | 11.94                          | 0.42                           | 18.26 | 0.61 | 8.93  | 9.30  | 0.18              | 0.78             | 0.04                          | 99.96  | 46.57 | 29.71   |
| 1664B5, 3S   | 48.43            | 0.57             | 9.70                           | 0.60                           | 17.74 | 0.55 | 13.18 | 8.41  | 0.08              | 0.46             | 0.01                          | 99.72  | 56.98 | 32.32   |



Table 1. *Continued.* Averaged compositions of individual glassy fragments and spherules in howardites. Values are in wt%.

| #   | SiO <sub>2</sub> | TiO <sub>2</sub> | Al <sub>2</sub> O <sub>3</sub> | Cr <sub>2</sub> O <sub>3</sub> | FeO   | MnO  | MgO   | CaO   | Na <sub>2</sub> O | K <sub>2</sub> O | P <sub>2</sub> O <sub>5</sub> | Total  | Mg#   | FeO/MnO |
|---|------------------|------------------|--------------------------------|--------------------------------|-------|------|-------|-------|-------------------|------------------|-------------------------------|--------|-------|---------|
| 1664B6, 1S  | 53.57            | 0.40             | 10.10                          | 0.47                           | 11.46 | 0.40 | 16.89 | 6.18  | 0.14              | 1.06             | 0.01                          | 100.68 | 72.43 | 28.65   |
| NWA 1664, crystal-rich glass (1664B3, 3)                      |                  |                  |                                |                                |       |      |       |       |                   |                  |                               |        |       |         |
| Glass   | 49.85            | 0.53             | 14.86                          | 0.39                           | 12.68 | 0.47 | 7.74  | 11.77 | 0.31              | 0.65             | 0.05                          | 99.30  | 52.09 | 27.04   |
| Opx (core)  | 54.75            | 0.12             | 1.57                           | 0.95                           | 11.50 | 0.54 | 28.96 | 1.05  | 0.00              | 0.00             | 0.01                          | 99.45  | 81.78 | 21.32   |
| Opx (rim)   | 51.24            | 0.19             | 4.03                           | 2.11                           | 14.58 | 0.68 | 23.19 | 3.10  | 0.01              | 0.01             | 0.01                          | 99.15  | 73.93 | 21.36   |
| Ol (core)   | 36.36            | 0.04             | 0.01                           | 0.02                           | 31.62 | 0.65 | 31.47 | 0.08  | 0.00              | 0.00             | 0.02                          | 100.27 | 63.95 | 48.97   |
| Ol (rim)  | 36.56            | 0.02             | 0.04                           | 0.08                           | 31.20 | 0.62 | 31.40 | 0.06  | 0.00              | 0.04             | 0.02                          | 100.04 | 64.20 | 50.54   |
| NWA 1664, composite spherule (1664B1, 1S)                     |                  |                  |                                |                                |       |      |       |       |                   |                  |                               |        |       |         |
| <i>Mafic glasses</i>  |                  |                  |                                |                                |       |      |       |       |                   |                  |                               |        |       |         |
| 1664B1, 1 S, core   | 51.10            | 0.73             | 13.38                          | 0.45                           | 13.17 | 0.47 | 8.34  | 10.91 | 0.20              | 1.41             | 0.01                          | 100.17 | 53.04 | 28.02   |
| 1664B1, 1 S, rim  | 49.82            | 0.72             | 13.17                          | 0.43                           | 15.52 | 0.54 | 7.72  | 10.82 | 1.21              | 0.06             | 0.07                          | 100.08 | 47.00 | 28.74   |
| <i>Felsic glass</i>   |                  |                  |                                |                                |       |      |       |       |                   |                  |                               |        |       |         |
| High K (n=11)   | 66.41            | 1.04             | 17.87                          | 0.26                           | 1.97  | 0.08 | 0.21  | 4.99  | 0.56              | 5.80             | 0.01                          | 99.20  | 16.07 | 24.63   |
| Low K (n=2)   | 65.36            | 1.11             | 18.96                          | 0.49                           | 1.96  | 0.05 | 0.19  | 7.04  | 0.61              | 3.95             | 0.00                          | 99.72  | 14.58 | 39.20   |
| NWA 1664, composite spherule (1664B7, 2S)                     |                  |                  |                                |                                |       |      |       |       |                   |                  |                               |        |       |         |
| Glass 1   | 48.83            | 0.64             | 12.30                          | 0.49                           | 17.30 | 0.51 | 9.20  | 10.48 | 0.25              | 0.37             | 0.05                          | 100.42 | 48.66 | 34.16   |
| Glass 2   | 49.78            | 0.65             | 12.19                          | 0.51                           | 17.07 | 0.57 | 9.36  | 9.06  | 0.16              | 1.32             | 0.08                          | 100.76 | 49.42 | 29.91   |
| NWA 1769, fusion crust, spherules (S) or glassy fragments (F) |                  |                  |                                |                                |       |      |       |       |                   |                  |                               |        |       |         |
| 1769A, fusion crust   | 49.06            | 0.54             | 10.47                          | 0.36                           | 18.69 | 0.57 | 10.34 | 8.74  | 0.34              | 0.03             | 0.04                          | 99.18  | 49.65 | 32.79   |
| 1769A, 1 S  | 48.27            | 0.63             | 10.81                          | 0.44                           | 18.80 | 0.55 | 11.63 | 8.90  | 0.14              | 0.28             | 0.01                          | 100.46 | 52.43 | 34.18   |
| 1769A, 2 S  | 48.45            | 0.46             | 7.71                           | 0.69                           | 22.50 | 0.41 | 15.43 | 2.12  | 0.22              | 2.33             | 0.02                          | 100.34 | 55.01 | 54.88   |
| 1769A, 3 S  | 49.42            | 0.50             | 8.44                           | 0.69                           | 17.20 | 0.54 | 16.03 | 6.65  | 0.05              | 0.37             | 0.01                          | 99.90  | 62.42 | 31.85   |
| 1769A, 4 S  | 45.89            | 0.63             | 10.39                          | 0.49                           | 23.09 | 0.53 | 11.84 | 4.89  | 0.29              | 1.79             | 0.01                          | 99.84  | 47.75 | 43.57   |
| 1769A, 5 S  | 49.83            | 0.55             | 9.24                           | 0.57                           | 16.36 | 0.61 | 13.11 | 8.67  | 0.10              | 0.65             | 0.03                          | 99.72  | 58.81 | 26.82   |
| 1769A, 6 S  | 50.51            | 0.67             | 12.01                          | 0.41                           | 15.79 | 0.55 | 8.45  | 9.48  | 0.20              | 1.48             | 0.01                          | 99.56  | 48.82 | 28.71   |
| 1769A, 8S   | 49.44            | 0.91             | 12.10                          | 0.35                           | 19.77 | 0.64 | 5.95  | 10.41 | 0.27              | 0.60             | 0.02                          | 100.46 | 34.92 | 31.07   |
| 1769B, 1 S  | 49.22            | 0.58             | 11.25                          | 0.48                           | 17.69 | 0.61 | 10.00 | 8.80  | 0.14              | 1.10             | 0.04                          | 99.91  | 50.19 | 29.00   |
| 1769B, 2 S  | 49.88            | 0.59             | 11.01                          | 0.49                           | 17.00 | 0.58 | 10.50 | 8.73  | 0.14              | 0.92             | 0.01                          | 99.85  | 52.39 | 29.31   |
| 1769B, 3 S  | 49.52            | 0.57             | 10.80                          | 0.29                           | 21.34 | 0.55 | 8.72  | 6.05  | 0.26              | 1.83             | 0.00                          | 99.93  | 42.13 | 38.80   |
| 1769B, 4 F  | 50.61            | 0.61             | 11.74                          | 0.49                           | 16.83 | 0.53 | 10.56 | 8.47  | 0.29              | 0.17             | 0.03                          | 100.33 | 52.80 | 31.75   |
| 1769B, 5 F  | 49.35            | 0.88             | 12.21                          | 0.31                           | 19.42 | 0.59 | 6.14  | 10.57 | 0.25              | 0.70             | 0.04                          | 100.46 | 36.03 | 32.92   |
| 1769C, 1 S  | 49.94            | 0.56             | 9.53                           | 0.62                           | 17.03 | 0.66 | 12.99 | 7.25  | 0.11              | 0.78             | 0.01                          | 99.48  | 57.61 | 25.80   |
| NWA 1769, spherule with an orthopyroxene nucleus (1769C, 2S)  |                  |                  |                                |                                |       |      |       |       |                   |                  |                               |        |       |         |
| Glass   | 49.62            | 0.62             | 11.72                          | 0.54                           | 16.75 | 0.61 | 9.53  | 9.14  | 0.16              | 1.21             | 0.05                          | 99.95  | 50.35 | 27.46   |
| Opx   | 54.68            | 0.06             | 0.73                           | 0.61                           | 15.02 | 0.50 | 27.13 | 1.14  | 0.01              | 0.00             | 0.02                          | 99.90  | 76.30 | 30.25   |
| LAP 04838, glass fragment                                     |                  |                  |                                |                                |       |      |       |       |                   |                  |                               |        |       |         |
| LAP, 1 F  | 49.21            | 0.85             | 11.19                          | 0.41                           | 18.26 | 0.60 | 8.33  | 9.95  | 0.18              | 0.72             | 0.09                          | 99.79  | 44.84 | 30.33   |
| LAP 04838, crystal-rich glass fragment                        |                  |                  |                                |                                |       |      |       |       |                   |                  |                               |        |       |         |
| LAP, 2 F  | 48.44            | 0.96             | 11.63                          | 0.37                           | 18.99 | 0.66 | 7.18  | 10.20 | 0.43              | 0.50             | 0.09                          | 99.45  | 40.26 | 28.75   |
| Opx1 (core)   | 50.82            | 0.45             | 3.88                           | 1.26                           | 17.86 | 0.62 | 21.49 | 3.53  | 0.02              | 0.01             | 0.01                          | 99.95  | 68.20 | 28.61   |
| Opx2 (core)   | 50.46            | 0.40             | 4.08                           | 1.38                           | 18.59 | 0.64 | 21.31 | 3.03  | 0.03              | 0.00             | 0.00                          | 99.92  | 67.15 | 29.10   |
| Opx2 (rim)  | 49.00            | 0.91             | 11.80                          | 0.34                           | 17.19 | 0.61 | 7.75  | 10.01 | 0.60              | 0.37             | 0.06                          | 98.64  | 44.57 | 28.20   |
| Pl  | 46.04            | 0.03             | 33.28                          | 0.00                           | 0.40  | 0.06 | 0.04  | 17.27 | 1.68              | 0.07             | 0.01                          | 98.88  |       |         |
| Px (low Ca)   | 50.18            | 0.37             | 0.57                           | 0.29                           | 30.98 | 0.94 | 15.20 | 1.40  | 0.02              | 0.00             | 0.00                          | 99.95  | 46.66 | 32.85   |
| Px (high Ca)  | 48.81            | 0.92             | 2.42                           | 1.10                           | 14.56 | 0.51 | 12.03 | 17.92 | 0.17              | 0.00             | 0.02                          | 98.46  | 59.56 | 28.72   |

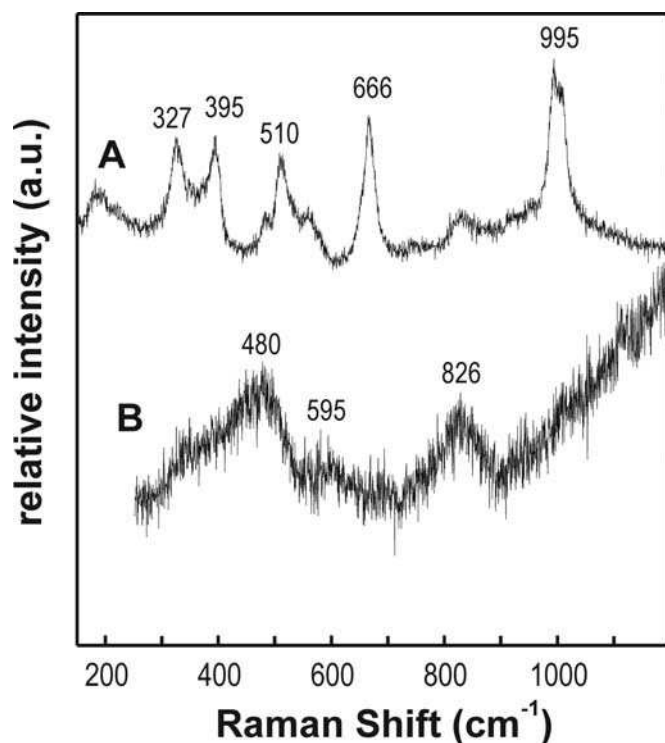


Fig. 7. Raman spectra recorded on two locations of the broken impact spherule shown in Figs. 3 and 4. Spectrum A has been obtained in the mafic glass poor in Na and enriched in K. The bands are characteristic of clinopyroxene. The spectrum bears also features of a silicate glass confirming the intermix of glass and crystallites. Spectrum B has been recorded in the felsic glass forming the K-rich strip. The spectrum is that of a pure glass with no trace of crystalline phases. The broad bands are characteristic of silica-rich glass.

have been occasionally observed in terrestrial impactites, and were ascribed to the contribution of alkali-rich liquids or seawater (Grieve 1978). Such an explanation is, of course, not applicable to the case of a dry body such as Vesta. Alternatively, impactites can be enriched in K via volatilization/condensation processes during crater formation (Yakovlev and Parfenova 1980). The latter mechanism could be operative on Vesta, and would result in selective enrichments and losses of elements depending on differences in their volatilization and condensation temperatures. However, it is not clear that such processes can account for a large K enrichment in impacted lithologies (one or two orders of magnitude in order to explain the compositions of the K-rich glasses). On the Moon, where rocks have suffered the effects of many impact events in a dry and airless environment like Vesta, Si-, Na-, K-, P-, and S-rich condensates have been observed in soils, but are generally small (<400 nm) and scarce (Keller and McKay 1992). Among the thousands of lunar impact glasses that have been analyzed so far, only a few display  $K_2O$  abundances up to 1 wt%. In these cases, K-rich condensates are not required to explain the high K concentrations, which

can be better rationalized by the involvement of K-rich lithologies, KREEP or less commonly granites (Lindstrom et al. 1991; Zellner et al. 2002; Zeigler et al. 2006). Alternatively, a K-enrichment in impact glasses is possible if the target is only partially melted, and if K is concentrated in the most fusible fraction. Such a process explains the composition of the glasses found in the so-called agglutinates (aggregates found in the lunar regolith, that consist of mineral, lithic and glass fragments cemented together by a glass and interpreted as impact-fused soil). They display generally enrichments in Al, Ca, Na, and K, and depletions in Mg, Fe, Mn in comparison to the bulk soil composition (e.g., Papike et al. 1982; Taylor et al. 2001). Indeed, the chemical compositions of the agglutinitic glasses approach the bulk composition of the finer fractions of the soils, which are enriched in the most friable (and fusible) components, namely feldspar and mesostasis. It is now accepted that agglutinitic glasses formed chiefly from the fusion of these finest fractions ( $F^3$  model, Papike et al. 1981; Basu et al. 2002). Their enrichments in Ca, Na, and K are linked to the composition of the feldspar fraction, and the latter is not particularly K-rich. Thus, the K abundances in agglutinitic glasses are generally low ( $K_2O < 0.5$  wt%, e.g., Papike et al. 1982; Taylor et al. 2001 and references therein). Although the  $F^3$  model could be effective on Vesta, such a process cannot account for the high-K abundances measured in glasses during the course of the study. The feldspar grains found in howardites are essentially eucritic plagioclases. Like the feldspars found in lunar soils, they are Ca-rich, in the range of bytownite to anorthite and have low K concentrations. Thus, if this process was operative on Vesta, it would have produced glasses with a range of K abundances similar to the lunar agglutinate one. Moreover, impact spherules and glass fragments are certainly not produced by the same processes as agglutinates. Hence, we will not further consider this possibility.

The compositions of the glasses found in the howardites have been plotted in a  $K_2O/CaO$  versus  $Al_2O_3/CaO$  plot (Fig. 12), and this diagram has important implications. Al and Ca are both refractory elements (e.g., Delano et al. 1981). Consequently, the  $Al_2O_3/CaO$  will not be significantly fractionated by impact melting. On the other hand, the  $K_2O/CaO$  ratio is highly sensitive to possible loss of K during melting, or enrichment in K via volatilization/condensation processes. A selective K-enrichment would result in an erratic behavior of K, and in a decoupling of K with respect to refractory elements, such as Fe, Al, or Ca (Delano et al. 1981). A very good correlation is obtained for the NWA 1664 and NWA 1769 glasses in the  $K_2O/CaO$  versus  $Al_2O_3/CaO$  plot. This relationship rules out condensation processes and strongly suggests the presence of K-rich components in their source region (Fig. 12). This conclusion is strengthened by the occurrence of the unmixed felsic melt in a spherule whose composition can potentially explain part of the scattering of

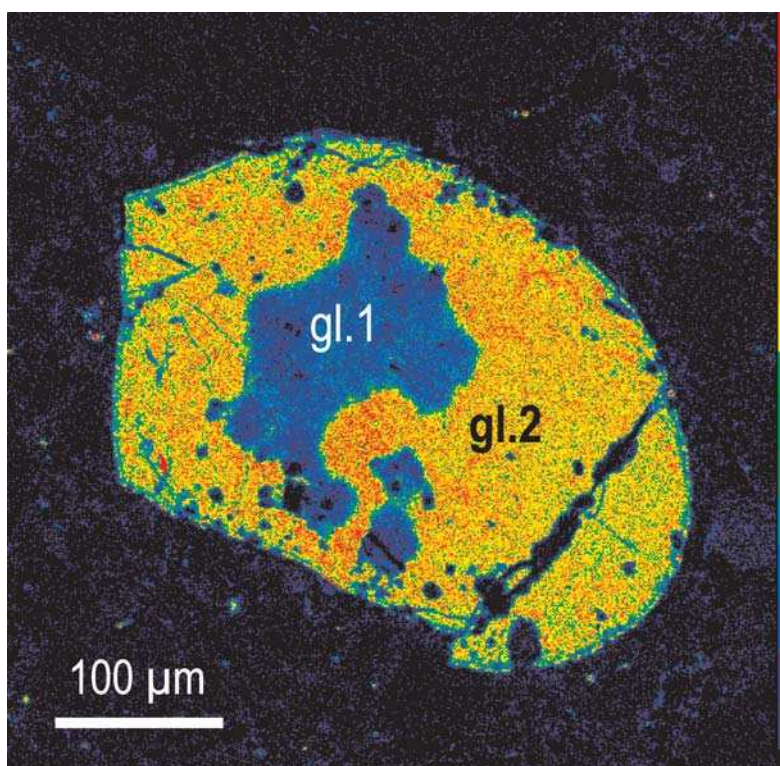


Fig. 8. K map of an impact spherule found in NWA 1664 (#1664B7,2S) that contains two basic K-rich glasses ( $K_2O = 0.37$  and  $1.32$  wt% for glass 1 and glass 2, respectively).

the data outside of the generally accepted HED field (Figs. 11 and 12).

Glasses are the only K-rich components present in the NWA 1664 and NWA 1769 howardites. Thus, unlike the low-K impact spherules found in the Bununu, Kapoeta, and Yamato howardites, the NWA 1664 and NWA 1769 glasses could not have formed by the melting of a source similar to their host breccias, nor from any combination of the known HED meteorites. Because of their high-K abundances, they necessarily originate from terranes not sampled, or not yet recognized, in HED meteorites.

The proportions of the different lithologies that were involved during the genesis of the impact melts can be estimated with mixing calculations, but are highly dependent on the chosen endmember compositions (Koeberl 2007). In order to estimate the proportions of the main eucritic and diogenitic lithologies involved during the genesis of the impact glasses found in howardites, we have performed mixing calculations using the Mona program (Metzner and Grimmeisen 1990). Usui and McSween (2007) have shown that combinations of three endmembers, namely, a diogenite (e.g., Shalka), a cumulate eucrite (e.g., Serra de Magé), and a low-Mg eucrite (e.g., Nuevo Laredo), reproduce all the major element abundances of HED meteorites satisfactorily (Usui and McSween 2007). Therefore, we have selected these endmembers for our calculations. Very good fits are obtained in the case of low-

K impact glasses, indicating that impact induced vapor fractionation effects, if any, are negligible. Examples of fits are given in Table 2, and the results are plotted in a ternary plot and compared with howardites (Fig. 13).

In the case of the high-K spherules, the  $K_2O/CaO$  and  $FeO/CaO$  versus  $Al_2O_3/CaO$  plots infer the involvement of one or more additional components significantly outside the chemical field of the HED (Fig. 12). A felsic endmember with the composition of the felsic glass found in a NWA 1664 can partly account for the high-K abundances of the spherules but not for the high  $FeO/CaO$  ratios shown by some of them. We have tentatively performed a series of least square calculations using a variety of HED lithologies and the felsic melt found in NWA 1664, but unfortunately no conclusive results have been obtained, suggesting that the selected endmembers were inappropriate. Better estimations of the proportions of the different lithologies involved during the genesis of the glasses must await new discoveries of high-K lithologies in HED meteorites.

A question of major importance concerns the origin or source of the felsic glass found in a NWA 1664 spherule fragment. One may argue that it formed from a fragment of mesostasis from a eucrite. This is unlikely because these mesostases do not show high-K concentrations, and K-feldspar has been observed in one case only (Barrat et al. 2007). The felsic glass is more likely an impact glass formed

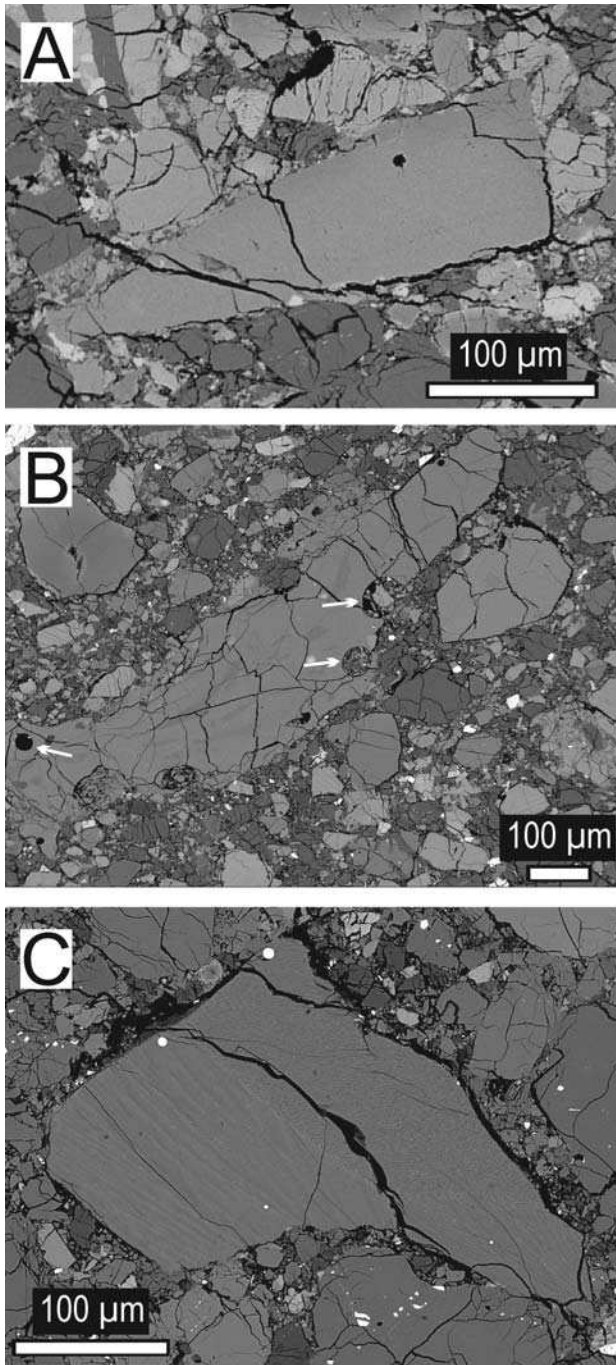


Fig. 9. Backscattered electron images of glass fragments from howardites. A) Vitreous fragment from LAP 04838. B) Vesicular glass fragment from NWA 1664. C) Glassy fragment from Y-7308 with very fine olivine and pyroxene crystals.

at the expense of a K-rich [granitic] or [felsic] clast present in the Vesta regolith. Interestingly, a small felsic glass with a much lower  $K_2O$  abundance (1 wt% only) was previously described in a diagenetic breccia (Takeda 1986), and confirms that acidic melts have been generated by the magmatic activity on Vesta.

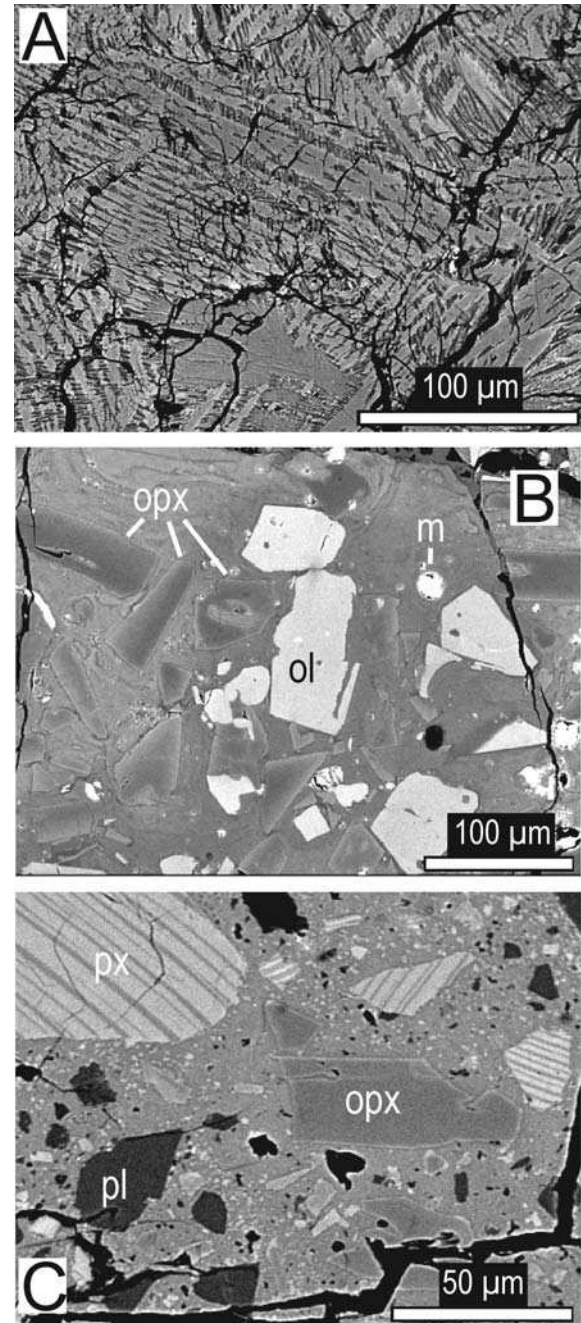


Fig. 10. Backscattered electron images of glass fragments from howardites. A) Skeletal pyroxene crystals in a glassy fragment from LAP 04838. B) Crystal-rich fragment from NWA 1664 (ol: olivine, opx: low-Ca pyroxene, m: metal). C) Crystal rich fragment from LAP 04838 (px: equilibrated eucritic pyroxene, pl: plagioclase, opx: low-Ca pyroxene).

Direct evidence of extraterrestrial rocks resembling granites is exceedingly rare. For example, rare iron meteorites display some inclusions that contain K-feldspar or K-rich glasses (e.g., Mittlefehldt et al. [1998]; Ruzicka et al. [2006]). Four small [granitic] clasts have been found in some LL chondritic breccias (Bischoff et al. [1993]; King



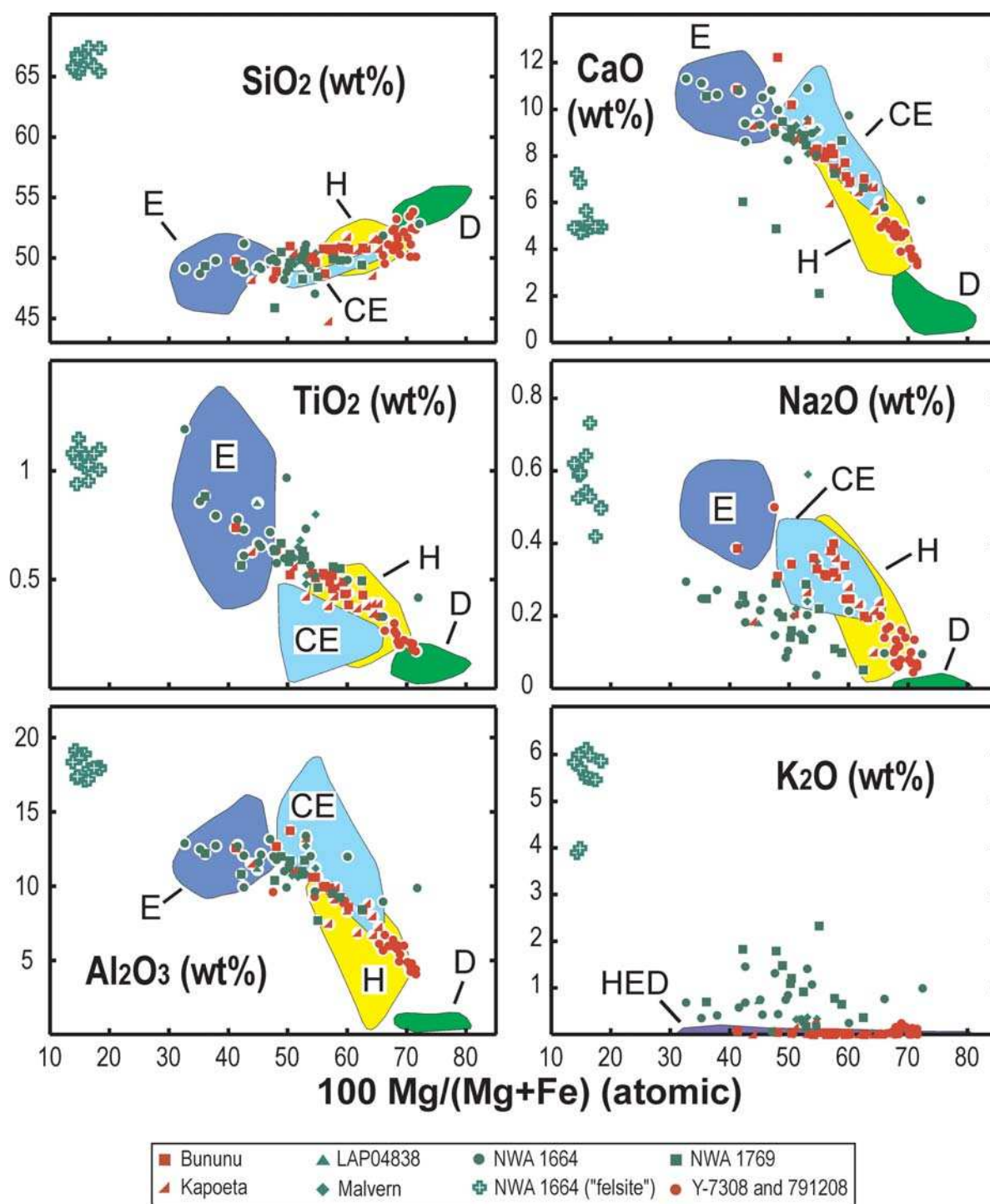


Fig. 11. SiO<sub>2</sub>, TiO<sub>2</sub>, Al<sub>2</sub>O<sub>3</sub>, CaO, Na<sub>2</sub>O, and K<sub>2</sub>O (wt%) versus 100 × Mg/(Mg + Fe) (atomic) plots for impact glasses from howardites (Noonan [1974]; Desnoyers and Jérôme [1977]; Yagi et al. [1978]; Hewins and Klein [1978]; Klein and Hewins [1979]; Noonan et al. [1980]; Delaney et al. [1982]; Ikeda and Takeda [1984], and this study). The fields for eucrites (E), cumulate eucrites (CE), diogenites (D), and howardites (H) are drawn from a compilation of literature data (see references in Mittlefehldt et al. [1998] and Barrat et al. [2007, 2008]).

et al. [2005]; Sokol et al. [2007]). The other known extraterrestrial granites were collected on the Moon during the Apollo missions (Papike et al. 1998). All lunar granites analyzed so far are very small fragments (the largest weighs

only 1.7 g) characterized by high SiO<sub>2</sub> (60 to 74 wt%) and K<sub>2</sub>O (2 to 10.4 wt%), and low Na<sub>2</sub>O (0.4 to 1.9 wt%) (Papike et al. 1998). Interestingly, the NWA 1664 glass resembles the lunar samples, but exhibits much higher

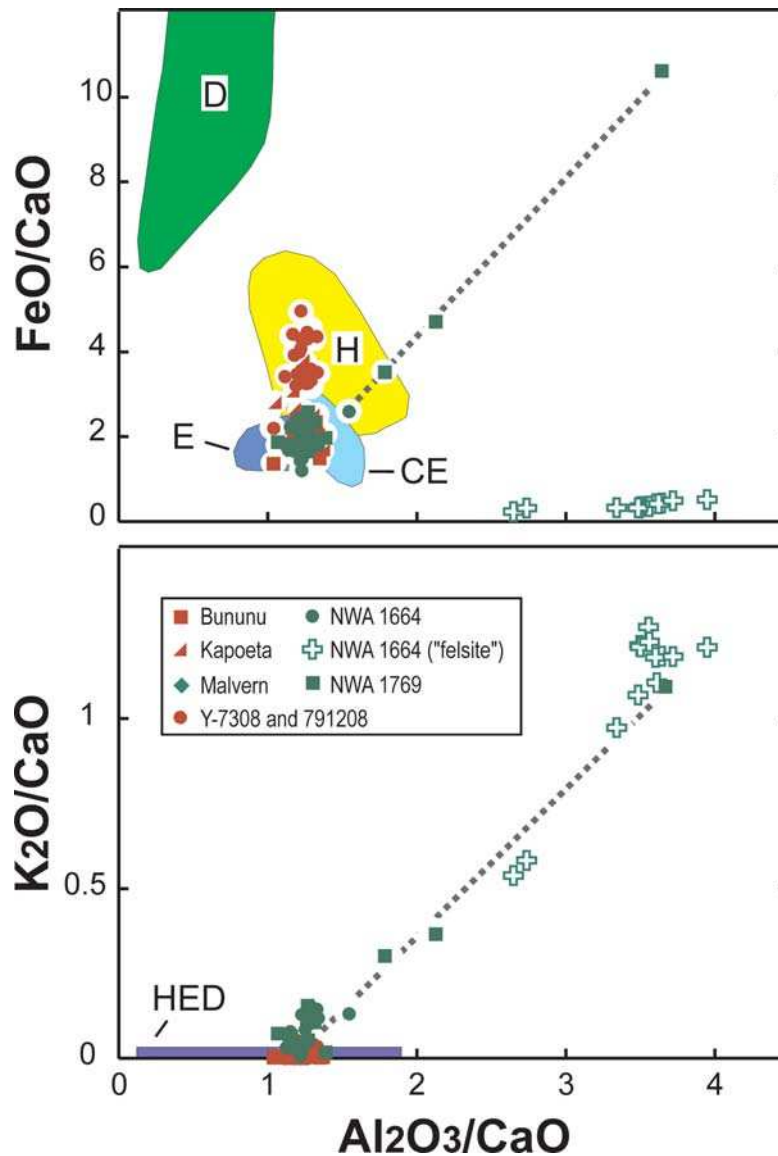


Fig. 12.  $\text{FeO}/\text{CaO}$ , and  $\text{K}_2\text{O}/\text{CaO}$  versus  $\text{Al}_2\text{O}_3/\text{CaO}$  (wt%/wt%) plots for impact glasses from howardites (Noonan [1974], Desnoyers and Jérôme [1977]; Yagi et al. [1978]; Hewins and Klein [1978]; Klein and Hewins [1979]; Noonan et al. [1980]; Delaney et al. [1982]; Ikeda and Takeda [1984], and this study). The fields for eucrites (E), cumulate eucrites (CE), diogenites (D), and howardites are drawn from a compilation of literature data (see references in Mittlefehldt et al. [1998] and Barrat et al. [2007, 2008]). The dotted line is the trend defined by the K-rich spherules.

$\text{Al}_2\text{O}_3$  abundances (about 18 wt% compared to  $8.8 \pm 3$  wt% in the lunar granites).

The rare lunar granites demonstrate that felsic melts can be generated on a dry planetary body, but their origin is still the subject of debate. It has been proposed that these melts result from extreme magma differentiation involving silicate liquid immiscibility (Papike et al. 1998). If this process was operative on the Moon, it could also be on Vesta. Indeed, extreme crystallization of a eucritic melt has been experimentally performed, and a K-rich felsic melt generated by silicate liquid immiscibility was obtained (Powell et al. 1980). Alternatively, remelting of the crust produced by

basaltic underplating could have generated felsic or granitic magmas on the Moon (Hagerty et al. 2006). On Vesta, remelting of the crust could have certainly occurred but was unable to generate directly K-rich acidic melts (Barrat et al. 2007).

## CONCLUSIONS

The K-rich impact glasses found in howardites suggest that the magmatic activity, which built Vesta's crust, was particularly complex. It is almost certain that the rocks that outcrop on this body are not restricted to mafic cumulates and

Table 2. Comparison of average glass compositions (this study) with those obtained from the mixing calculations using the given endmembers (oxides in wt%). The proportions of endmembers are given in wt%.

| SiO <sub>2</sub>  | TiO <sub>2</sub> | Al <sub>2</sub> O <sub>3</sub> | Cr <sub>2</sub> O <sub>3</sub> | FeO   | MnO  | MgO   | CaO   | Na <sub>2</sub> O | K <sub>2</sub> O |
|---|------------------|--------------------------------|--------------------------------|-------|------|-------|-------|-------------------|------------------|
| <b>Endmembers</b>   |                  |                                |                                |       |      |       |       |                   |                  |
| <i>Shalka</i>   |                  |                                |                                |       |      |       |       |                   |                  |
| 53.15   | 0.06             | 0.62                           | 1.44                           | 16.79 | 0.57 | 26.57 | 0.75  | 0.04              | 0.00             |
| <i>Nuevo Laredo</i>   |                  |                                |                                |       |      |       |       |                   |                  |
| 48.59   | 0.92             | 12.16                          | 0.30                           | 20.56 | 0.62 | 5.61  | 10.72 | 0.47              | 0.06             |
| <i>Serra de Magé</i>  |                  |                                |                                |       |      |       |       |                   |                  |
| 48.64   | 0.13             | 14.84                          | 0.63                           | 14.44 | 0.48 | 10.73 | 9.83  | 0.25              | 0.01             |
| <b>Mixing calculations</b>  |                  |                                |                                |       |      |       |       |                   |                  |
| <i>Bununu</i> (average, <i>n</i> = 6)   |                  |                                |                                |       |      |       |       |                   |                  |
| 49.88   | 0.54             | 10.98                          | 0.45                           | 17.12 | 0.55 | 11.02 | 9.13  | 0.31              | 0.04             |
| <i>Model</i> (16.51 % <i>Shalka</i> + 42.91% <i>Nuevo Laredo</i> + 41.16 <i>Serra de Magé</i> ) |                  |                                |                                |       |      |       |       |                   |                  |
| 49.65   | 0.46             | 11.43                          | 0.63                           | 17.54 | 0.56 | 11.21 | 8.77  | 0.31              | 0.03             |
| <i>Kapoeta</i> (average, <i>n</i> = 8)  |                  |                                |                                |       |      |       |       |                   |                  |
| 49.84   | 0.45             | 9.57                           | 0.56                           | 17.76 | 0.50 | 13.47 | 7.55  | 0.25              | 0.04             |
| <i>Model</i> (29.79% <i>Shalka</i> + 40.95 <i>Nuevo Laredo</i> + 29.21 <i>Serra de Magé</i> )   |                  |                                |                                |       |      |       |       |                   |                  |
| 49.94   | 0.43             | 9.50                           | 0.74                           | 17.64 | 0.56 | 13.35 | 7.48  | 0.28              | 0.03             |
| <i>Y-7308</i> (average, <i>n</i> = 7)   |                  |                                |                                |       |      |       |       |                   |                  |
| 52.25   | 0.21             | 5.38                           | 1.08                           | 15.77 | 0.52 | 20.37 | 4.25  | 0.10              | 0.08             |
| <i>Model</i> (63.69 <i>Shalka</i> + 3.67 <i>Nuevo Laredo</i> + 33.45 <i>Serra de Magé</i> )     |                  |                                |                                |       |      |       |       |                   |                  |
| 51.90   | 0.12             | 5.81                           | 1.14                           | 16.28 | 0.54 | 20.72 | 4.16  | 0.13              | 0.01             |

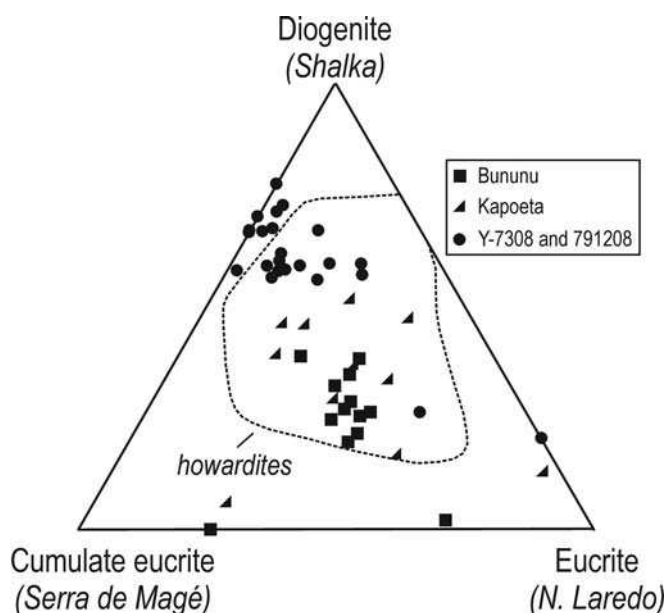


Fig. 13. Results of mixing calculations for the various low-K spherules and glassy fragments (Noonan 1974; Hewins and Klein 1978; Yagi et al. 1978; Klein and Hewins 1979; Noonan et al. 1980; Ikeda and Takeda 1984, and this study).

basaltic flows, but that more evolved and more K-rich lithologies than those actually known in the HED collection are exposed somewhere on Vesta. In this respect, our current sampling of the surface of Vesta (the HED) is necessarily incomplete. For example, cosmic-ray exposure ages for the HED suggest that all samples can be associated with one of only five impact events (Eugster and Michel 1995; Welten

et al. 1997). In other words, only five localities at the surface of Vesta have been sampled, a number probably not sufficient to describe the geological diversity of the entire surface of the body. In September 2007, the Dawn spacecraft was launched to the asteroid belt and will begin studying Vesta and Ceres in 2011 (Russell et al. 2007). The planned remote sensing studies should allow the identification of chemically different areas on Vesta, and may help pinpoint the source regions of the K-rich impact glasses.

**Acknowledgments**—Brigitte Zanda (NWA 1664 and NWA 1769), Ahmed Pani (NWA 1664), Philippe Thomas (NWA 1769), the Meteorite Working Group (LAP 04838), D. Brownlee (Kapoeta), the Arizona State University (Kapoeta), and the U.S. National Museum of Natural History (Bununu) are thanked for providing us the samples. The EPMA analyses of the Bununu and Kapoeta glasses were obtained when A. Yamaguchi was a post-doctoral fellow at the Hawai'i Institute of Geophysics and Planetology, University of Hawai'i, where his work was partially supported by a NASA Cosmochemistry grant for K. Keil (PI). The comments provided by F. Albarède, M. A. Gutscher, E. Scott, R. N. Taylor, and M. Toplis of an early version of the manuscript have significantly improved the text. We would like to thank C. Goodrich for the editorial handling and J. Boesenberg, A. Ruzicka, and the anonymous reviewers for their comments. This study was supported by Programme National de Planétologie de l'Institut National des Sciences de l'Univers. J. A. B. acknowledges Pascale Barrat for her help.

**Editorial Handling**—Dr. Cyrena Goodrich

## REFERENCES

- Arndt J., Engelhardt W. von, Gonzalez-Cabeza I., and Meier B. 1984. Formation of Apollo 15 green glass beads. *Journal of Geophysical Research* 89:C225–C232.
- Barrat J. A., Jambon A., Bohn M., Blichert-Toft J., Sautter V., Göpel C., Gillet Ph., Boudouma O., and Keller F. 2003. Petrology and geochemistry of the unbrecciated achondrite Northwest Africa 1240 (NWA 1240): An HED parent body impact melt. *Geochimica et Cosmochimica Acta* 67:3959–3970.
- Barrat J. A., Yamaguchi A., Greenwood R. C., Bohn M., Cotten J., Benoit M., and Franchi I. A. 2007. The Stannern trend eucrites: Contamination of main group eucritic magmas by crustal partial melts. *Geochimica et Cosmochimica Acta* 71:4108–4124.
- Barrat J. A., Yamaguchi A., Benoit M., Cotten J., and Bohn M. 2008. Geochemistry of diogenites: Still more diversity in their parental melts. *Meteoritics & Planetary Science* 43:1759–1775.
- Basu A., Wentworth S. J., and McKay D. S. 2002. Heterogeneous agglutinitic glass and the fusion of the finest fraction (F<sup>3</sup>) model. *Meteoritics & Planetary Science* 37:1835–1842.
- Bischoff A., Geiger T., Palme H., Spettel B., Schultz L., Scherer P., and Lkhamsuren J. 1993. Mineralogy, chemistry, and noble gas contents of Adzhi-Bogdo, an LL3–6 chondritic breccia with L-chondritic and granitoid clasts. *Meteoritics* 28:570–578.
- Boesenberg J. S. and Mandeville C. W. 2007. The driest glass in the solar system: Glass spherules in howardites (abstract). *Meteoritics & Planetary Science* 42:A20.
- Buchanan P. C., Lindstrom D. J., Mittlefehldt D. W., Koeberl C., Reimold W. U. 2000. The South African polymict eucrite Macibini. *Meteoritics & Planetary Science* 35:1321–1331.
- Delaney J. S., Prinz M., and Nehru C. E. 1982. Partial melt genesis for glassy clasts in basaltic achondrites (abstract). *Meteoritics* 17: 204–205.
- Delano J. W., Lindsley D. H., and Rudowski R. 1981. Glasses of impact origin from Apollo 11, 12, 15, and 16: Evidence for fractional vaporization and mare/highland mixing. Proceedings, 12th Lunar and Planetary Science Conference. pp. 339–370.
- Desnoyers C. and Jérôme J. Y. 1977. The Malvern howardite: A petrological and chemical discussion. *Geochimica et Cosmochimica Acta* 41:81–86.
- Donaldson C. H., Usselman T. M., Williams R. J., and Lofgren G. E. 1975. Experimental modeling of the cooling history of Apollo 12 olivine basalts. Proceedings, 6th Lunar Science Conference. pp. 843–869.
- Drake M. J. 2001. The eucrite/Vesta story. *Meteoritics & Planetary Science* 36:501–513.
- Engelhardt W. von, Arndt J., and Witzsche A. 1989. Al-rich pyroxenes: Metastable formation in supercooled lunar basaltic and terrestrial impact melts. 20th Lunar and Planetary Science Conference. pp. 266–267.
- Eugster O. and Michel Th. 1995. Common breakup events of eucrites, diogenites, and howardites and cosmic-ray production rates for noble gases in achondrites. *Geochimica et Cosmochimica Acta* 59:501–513.
- Faure F., Trolliard G., Nicollet C., and Montel J. M. 2003. A developmental model of olivine morphology as a function of the cooling rate and the degree of undercooling. *Contributions to Mineralogy and Petrology* 145:251–263.
- Fowler G. W., Papike J. J., Shearer C. K., and Spilde M. N. 1994. Diogenites as asteroidal cumulates. Insights from orthopyroxene major and minor element chemistry. *Geochimica et Cosmochimica Acta* 58:3921–3929.
- Grieve R. A. F. 1978. The melt rocks at Brent crater. Proceedings, 9th Lunar and Planetary Science Conference. pp. 2579–2608.
- Hagerty J. J., Lawrence D. L., Hawke B. R., Vaniman D. T., Elphic R. C., and Feldman W. C. 2006. Refined thorium abundances for lunar red spots: Implications for evolved, non-mare volcanism on the Moon. *Journal of Geophysical Research* 111, E06002, doi:10.1029/2005JE002592, 1–20.
- Hewins R. H. and Klein L. C. 1978. Provenance of metal and melt rock textures in the Malvern howardite. Proceedings, 9th Lunar and Planetary Science Conference. pp. 1137–1156.
- Ikeda Y. and Takeda H. 1984. Petrography and mineral compositions of the Yamato-7308 howardite. *Proceedings of the Ninth Symposium on Antarctic Meteorites*. pp. 149–183.
- Keller L. P. and McKay D. S. 1992. Micrometer-sized glass spheres in Apollo 16 soil 61181: Implications for impact volatilization and condensation. Proceedings, 22nd Lunar and Planetary Science Conference. pp. 137–141.
- King P. L., Dalby K. N., Russell S. D. J., Ireland T., McSween Jr. H. Y., and Bischoff A. 2005. Early solar system granites (abstract #5260). *Meteoritics & Planetary Science* 40:A82.
- Klein L. C. and Hewins R. H. 1979. Origin of impact melt rocks in the Bununu howardite. Proceedings, 10th Lunar and Planetary Science Conference. pp. 1127–1140.
- Koeberl C. 2007. The geochemistry and cosmochemistry of impacts. In *Meteorites, comets, and planets*, edited by Davis A. Treatise on Geochemistry, vol. 1. pp. 1–52.
- Kurat G., Varela M. E., Zinner E., Maruoka T., and Brandstätter F. 2003. Major, minor and trace elements in some glasses from the NWA 1664 howardite (abstract #1733). 34th Lunar and Planetary Science Conference. CD-ROM.
- Lindstrom M. M., Wentworth S. J., Martinez R. R., Mittlefehldt D. W., McKay D. S., Wang M. S., and Lipschutz M. E. 1991. Geochemistry and petrography of the MacAlpine Hills lunar meteorites. *Geochimica et Cosmochimica Acta* 55:3089–3103.
- McCoy T. J., Mittlefehldt D. W., and Wilson L. 2006. Asteroid differentiation. In *Meteorites and the early solar system II*, edited by Lauretta D. and McSween Jr. H. Y. Tucson: The University of Arizona Press. 735 p.
- Metzner C. and Grimmeisen W. 1990. MONA: A user-friendly computer-program for calculating the modal mineralogy of rocks from chemical analyses. *European Journal of Mineralogy* 2: 735–738.
- Mittlefehldt D. W. 1994. The genesis of diogenites and HED parent body petrogenesis. *Geochimica et Cosmochimica Acta* 58:1537–1552.
- Mittlefehldt D. W., McCoy T. J., Goodrich C. A., and Kracher A. 1998. Non-chondritic meteorites from asteroidal bodies. In *Planetary materials*, edited by Papike J. J. Reviews in Mineralogy and Geochemistry, vol. 36, chapter 4. Washington, D.C.: Mineralogical Society of America. pp. 1–95.
- Noonan A. F. 1974. Glass particles and shock features in the Bununu howardite. *Meteoritics* 9:233–242.
- Noonan A. F., Rajan S., Fredriksson K., and Nelen J. 1980. Chondrules in the Kapoeta and Bununu howardites. LPI Contribution #412. Houston: Lunar and Planetary Institute. pp. 139–140.
- Papike J. J., Ryder G., and Shearer C. K. 1998. Lunar samples. In *Planetary materials*, edited by Papike J. J. Reviews in Mineralogy and Geochemistry, vol. 36, chapter 5. Washington, D.C.: Mineralogical Society of America. pp. 1–234.
- Papike J. J., Simon S. B., White C., and Laul J. C. 1981. The relationship of the lunar regolith <10  $\mu$ m fraction and agglutinates, Part 1. A model for agglutinate formation and some indirect supportive evidence. Proceedings, 12th Lunar and Planetary Science Conference. pp. 409–420.
- Papike J. J., Simon S. B., and Laul J. C. 1982. The lunar regolith: Chemistry, mineralogy, and petrology. *Reviews of Geophysics and Space Physics* 20:761–826.



- Powell M. A., Walker D., and Hays J. F. 1980. Controlled cooling and crystallization of a eucrite: Microprobe studies. *Proceedings, 11th Lunar and Planetary Science Conference*. pp. 1153–1168.
- Russell C. T., Capaccioni F., Coradini A., De Sanctis M. C., Feldman W. C., Jaumann R., Keller H. U., McCord T. B., McFadden L. A., Mottola S., Pieters C. M., Prettyman T. H., Raymond C. A., Sykes M. V., Smith D. E., and Zuber M. T. 2007. Dawn mission to Vesta and Ceres. *Earth, Moon and Planets* 101, 65, doi: 10.1007/s11038-007-9151-9.
- Ruzicka A., Snyder G. A., and Taylor L. A. 2000. Crystal-bearing lunar spherules: Impact melting of the Moon's crust and implications for the origin of meteoritic spherules. *Meteoritics & Planetary Science* 35:173–192.
- Ruzicka A., Hutson M., and Floss C. 2006. Petrology of silicate inclusions in the Sombereite ungrouped iron meteorite: Implications for the origin of IIE-type silicate-bearing irons. *Meteoritics & Planetary Science* 41:1797–1831.
- Sokol A. K., Bischoff A., Marhas K. K., Mezger K., and Zinner E. 2007. Late accretion and lithification of chondritic parent bodies: Mg isotope studies on fragments from primitive chondrites and chondritic breccias. *Meteoritics & Planetary Science* 42:1291–1308.
- Sunshine J. M., Bus S. J., McCoy T. J., Burbine T. H., Corrigan C. M., and Binzel R. P. 2004. High-calcium pyroxene as an indicator of igneous differentiation in asteroids and meteorites. *Meteoritics & Planetary Science* 39:1343–1357.
- Takeda H. 1986. Mineralogy of Yamato-791073 with reference to crystal fractionation of the howardite parent body. *Proceedings, 16th Lunar and Planetary Science Conference, part 2. Journal of Geophysical Research* 91, B4:D355–D363.
- Taylor L. A., Pieters C. M., Keller L. P., Morris R. V., and McKay D. S. 2001. Lunar mare soils: Space weathering and the major effects of surface-correlated nanophase Fe. *Journal of Geophysical Research* 106, E11:27,985–27,999.
- Thompson A. B., Aerts M., and Hack A. C. 2007. Liquid immiscibility in silicate melts and related systems. In *Fluid-fluid interactions*, edited by Liebscher A. and Heinrich C. A. Reviews in Mineralogy and Geochemistry, vol. 65. Washington, D.C.: Mineralogical Society of America. pp. 99–127.
- Usui T. and McSween H. P. 2007. Geochemistry of 4 Vesta based on HED meteorites: Prospective study for interpretation of gamma ray and neutron spectra for the Dawn mission. *Meteoritics & Planetary Science* 42:255–269.
- Weidenschilling S. J. 2000. Formation of planetesimals and accretion of the terrestrial planets. *Space Science Reviews* 92: 295–310.
- Welten K. C., Lindner L., Van der Borg K., Loeken T., Scherer P., and Schultz L. 1997. Cosmic-ray exposure ages of diogenites and the recent collisional history of the howardite, eucrite and diogenite parent body/bodies. *Meteoritics & Planetary Science* 32:891–902.
- Yagi K., Lovering J., Shima M., and Okada A. 1978. Mineralogical and petrological studies of the Yamato meteorites, Yamato-7301(j), -7305(k), -7308(l) and -7303(m) from Antarctica. *Proceedings of the Second Symposium on Antarctic Meteorites*. pp. 121–141.
- Yakovlev O. I. and Parfenova O. V. 1980. The role of vaporization and condensation in the formation of the chemical composition of impactites. *Proceedings, 11th Lunar and Planetary Science Conference*. pp. 1285–1287.
- Zeigler R. A., Korotev R. L., Jolliff B. L., Haskin L. A., and Floss C. 2006. The geochemistry and provenance of Apollo 16 mafic glasses. *Geochimica et Cosmochimica Acta* 70: 6050–6067.
- Zellner N. E. B., Spudis P. D., Delano J. W., and Whittet D. C. B. 2002. Impact glasses from the Apollo 14 landing site and implications for regional geology. *Journal of Geophysical Research* 107:5102–5115.